Downloaded from orbit.dtu.dk on: Apr 18, 2024

DTU Library

Why the Coriolis force turns a wind farm wake to the right in the Northern Hemisphere

van der Laan, Paul; Sørensen, Niels N.

Published in:
Journal of Physics: Conference Series (Online)

Link to article, DOI:
10.1088/1742-6596/753/3/032031

Publication date:
2016

Document Version
Publisher's PDF, also known as Version of record

Link back to DTU Orbit

Citation (APA):
van der Laan, P., & Sørensen, N. N. (2016). Why the Coriolis force turns a wind farm wake to the right in the Northern Hemisphere. *Journal of Physics: Conference Series (Online)*, *753*, Article 032031. https://doi.org/10.1088/1742-6596/753/3/032031

General rights
Copyright and moral rights for the publications made accessible in the public portal are retained by the authors and/or other copyright owners and it is a condition of accessing publications that users recognise and abide by the legal requirements associated with these rights.

- Users may download and print one copy of any publication from the public portal for the purpose of private study or research.
- You may not further distribute the material or use it for any profit-making activity or commercial gain
- You may freely distribute the URL identifying the publication in the public portal

If you believe that this document breaches copyright please contact us providing details, and we will remove access to the work immediately and investigate your claim.

Why the Coriolis force turns a wind farm wake to the right in the Northern Hemisphere

M. P. van der Laan[1] **and N. N. Sørensen**[1]

[1]Technical University of Denmark, DTU Wind Energy, Risø Campus, Frederiksborgvej 399, 4000 Roskilde, Denmark

E-mail: plaa@dtu.dk

Abstract. The interaction between the Coriolis force and a wind farm wake is investigated by Reynolds-Averaged Navier-Stokes simulations, using two different wind farm representations: a high roughness and 5×5 actuator disks. Surprisingly, the calculated wind farm wake deflection is opposite in the two simulations. A momentum balance in the cross flow direction shows that the interaction between the Coriolis force and the 5×5 actuator disks is complex due to turbulent mixing of fresh momentum from above into the wind farm, which is not observed for the interaction between the Coriolis force and a roughness change.

1. Introduction

In recent years, wind farms have grown in size and are more frequently placed in wind farm clusters. This means that large scale effects are becoming more important for wind turbine wake interaction in wind farms, and especially for the interaction between wind farms. One large scale effect that is often neglected by wind farm modelers is the effect of the Coriolis force on wind turbine/farm wakes. In previous work, we have shown that the Coriolis force should not be neglected in Reynolds-Averaged Navier-Stokes simulations of a wind farm cluster consisting of two wind farms[1]. The deflection of the upstream wind farm wake resulted in a lower power production of the downstream wind farm, because the Coriolis force aligned the upstream wind farm wake towards the curved rows of the downstream wind farm. Note that a constant latitude was used, which means that the global turning of the Coriolis force was not modeled. In other words, only the interaction between the Coriolis force and local disturbances in the velocity field were investigated. In the present work, we will also use a constant latitude.

The literature does not agree on the turning direction of wind farm wakes caused by the Coriolis force. Volker et al.[2] showed that different mesoscale models can show wind farm wake deflection in opposite directions for the same test case. Mitraszewski[3] argued that a wind farm can be seen as a roughness change, and therefore the Coriolis force should turn the wind farm wake to the left (in the Northern Hemisphere), following Orr et al.[4]. On the contrary, we have shown in previous work that the Coriolis force turns a wind farm wake to the right (in the Northern Hemisphere), and we explained it as result of a stream-wise decreasing Coriolis force in the wake recovery region[1]. However, the present work shows that this effect is not the main reason for the wind farm wake to turn to the right. Our goal is to clarify why the Coriolis force turns a wind farm wake to the right in the Northern Hemisphere.

Content from this work may be used under the terms of the Creative Commons Attribution 3.0 licence. Any further distribution of this work must maintain attribution to the author(s) and the title of the work, journal citation and DOI.
Published under licence by IOP Publishing Ltd

2. Methodology

In order to understand the interaction between the Coriolis force and a wind farm wake, two RANS simulations of a simple rectangular wind farm of 5×5 NREL-5MW wind turbines[5] are carried out, where the wind farm is represented in two different ways:

(i) 25 wind turbines represented by actuator disks (ADs) with variable forces, without wake rotation[6, 7].

(ii) A high roughness of 1 m in the wind farm area.

The NREL-5MW wind turbine has a hub height and a rotor diameter (D) of 90 m and 126 m, respectively. The wind turbines spacing is set to 8D in both horizontal directions.

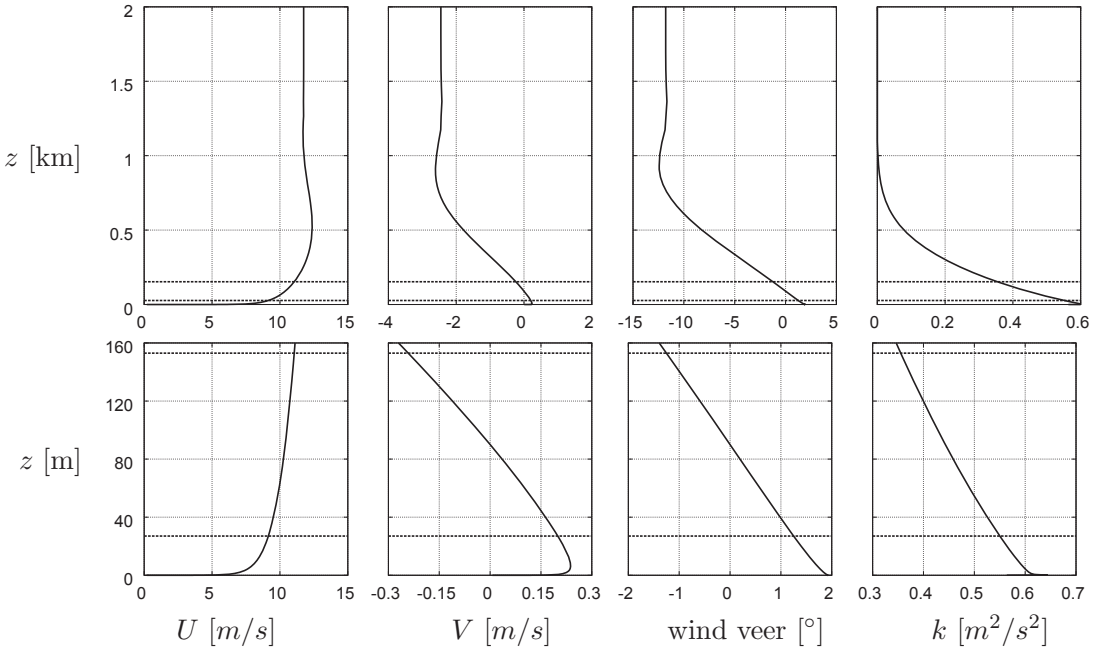

Figure 1. Rotated inlet profiles calculated by the precursor. Bottom plots are a zoomed view of the top plots. Rotor area is shown as black dashed lines.

The numerical setup of the RANS simulations with ADs including the Coriolis force is fully described in previous work[1], and we will briefly summarize it here. The simulations are carried out with the in-house flow solver EllipSys3D[8, 9]. The turbulence is modeled with a modified k-ε model that limits the boundary height through a global length scale limiter[10], and it includes a local length scale limiter that is necessary to resolve the near wind turbine wake properly[11]. The inflow profiles of the wind farm simulations are determined from a neutrally stratified precursor simulation, where the Coriolis force is balanced by a defined pressure gradient, both terms are implemented as a momentum source term S_v:

$$S_{v,x} = \rho f_c \left(V - V_G\right), \quad S_{v,y} = -\rho f_c \left(U - U_G\right), \tag{1}$$

with ρ as the air density, f_c as the Coriolis parameter set to 10^{-4} 1/s, U and V are the streamwise and lateral velocity components, and the subscript G denotes the geostrophic wind, which is set to 12 m/s. A uniform roughness length of 10^{-4} m is chosen. The precursor calculates a velocity of 10.4 m/s and a turbulence intensity of 5% at hub height, which represents off-shore conditions. The calculated profiles include wind veer, and are rotated to enforce a chosen row

aligned wind direction of 270° at hub height in the wind farm simulations. The rotated inflow profiles from the precursor simulation are shown in Figure 1. A wind veer of about 2.6° is present in the rotor area, as shown in one of the bottom plots of Figure 1.

The same numerical grid is used in both wind farm simulations. The domain definition including wind farm layout and boundary conditions (BC) is shown in Figure 2. The grid is Cartesian and represents a box-shaped domain with dimensions 2000D×1000D×20D, in stream-wise, lateral and vertical directions, respectively. The grid consist of 26 million cells, where the spacing in and around the wind farm (blue area of Figure 2) is D/8. In the green area of Figure 2, the grid cells are streched in the stream-wise direction towards a spacing of 1D, up to 396D ≈ 50 km downstream. The vertical resolution starts with a cell height of 0.5 m and it grows with height using an expansion ratio of about 1.1. The profiles from the precursor simulation are inserted at the at inlet BC, as shown in Figure 2. In addition, the top boundary of the domain is also an inlet BC. The lateral boundaries are periodic to account for wind veer. At the outlet BC, a fully developed flow is assumed. A rough wall BC [12] is placed at the bottom of the domain.

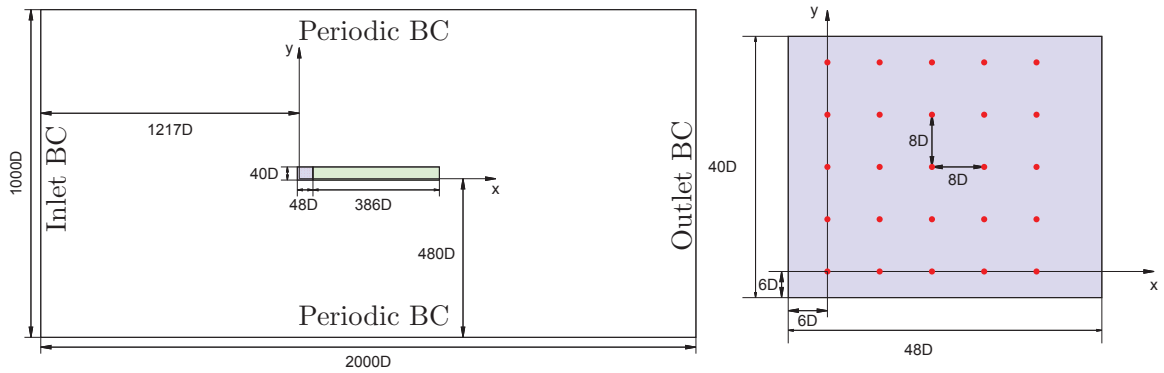

Figure 2. Domain definition and wind farm layout. Left: overview of domain, right: zoomed view. Red dots represent ADs. Spacing in blue and green areas are set to D/8 and D, respectively.

3. Results and Discussion

Figure 3 shows two contours plots of the stream-wise velocity, taken at hub height, for the two wind farm representations: 25 ADs and a high roughness. The x and y coordinates are normalized by the length or width of the wind farm $L_{WF} = 32D$. The simulation with 25 ADs shows five distinct merged wakes, while the simulation of the roughness change shows one wind farm wake structure. A contour line that represents 95% recovered velocity is shown in each plot of Figure 3. The contour line reveals that the wake of the wind farm represented by ADs is deflected towards the right, while the opposite is observed for the wind farm represented by a high roughness. The wind farm wake deflection is also visible in Figure 4, where the stream-wise velocity is plotted at five cross planes located at $x/L_{WF} = 0, 0.1, 1, 1.25, 2$, for both simulations.

3.1. Momentum balance

In this section, the observed wind farm wake deflection from Figures 3 and 4, is explained using a momentum balance.

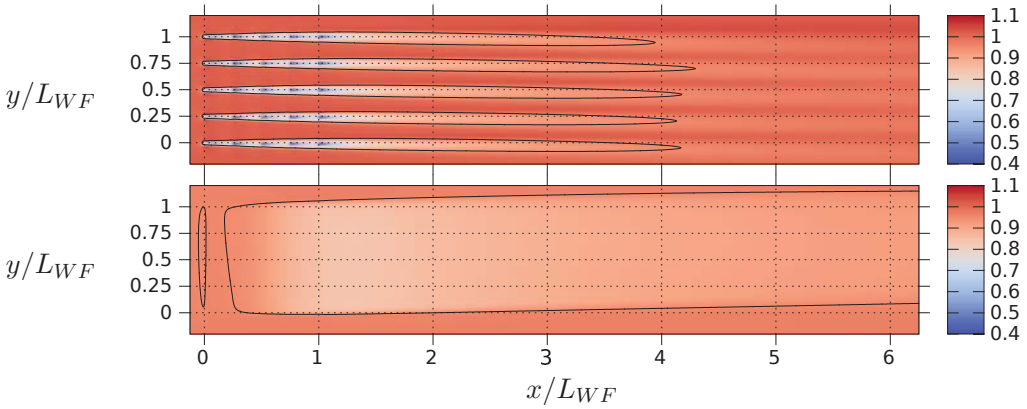

Figure 3. Stream-wise velocity at hub height, normalized by the free-stream. Top: Wind farm modeled with 25 ADs. Bottom: Wind farm modeled as a high roughness. Contour line represents 95% recovered velocity.

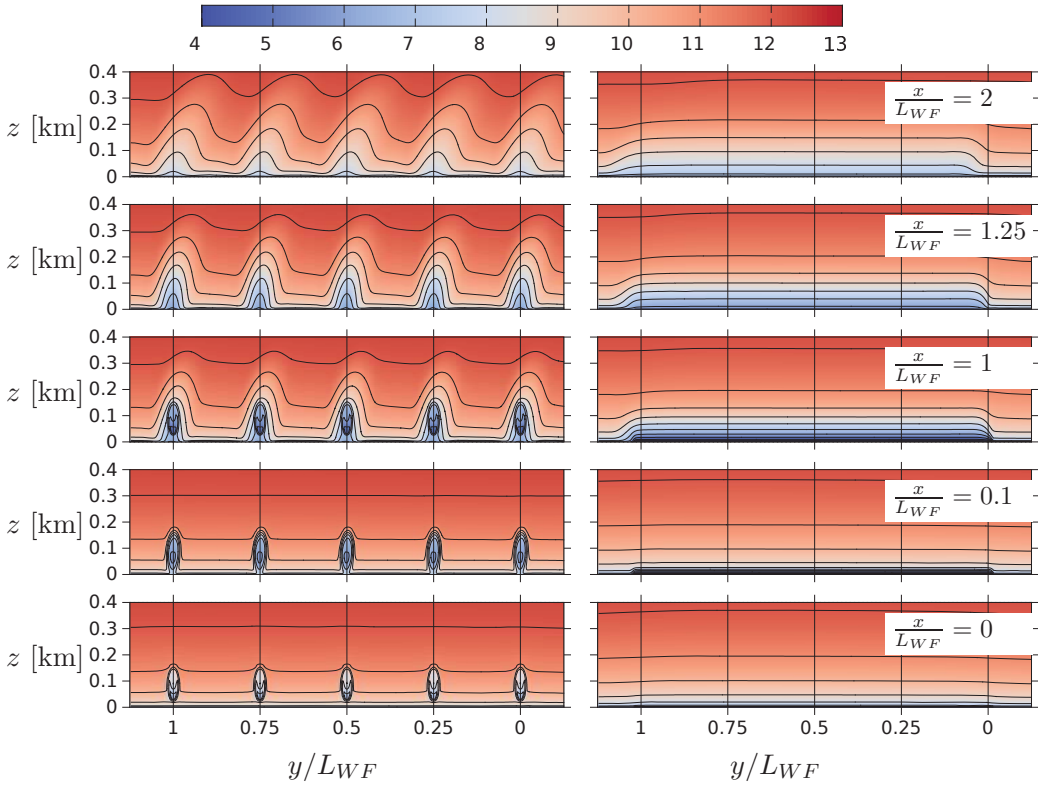

Figure 4. Stream-wise velocity at several downstream cross planes. Left: wind farm is represented by 25 ADs. Right: wind farm is represented by a high roughness. Wind farm ends at $x/L_{WF} = 1$.

The momentum equation can be written as:

$$\frac{DU_i}{Dt} = S_{AD,i} + \frac{1}{\rho}\left(S_{v,i} - \frac{\partial \widetilde{P}}{\partial x_i}\right) - \frac{\partial \overline{u_i' u_j'}}{\partial x_j} \tag{2}$$

Here, we neglect the molecular viscosity since it is much smaller than the eddy viscosity. $S_{AD,i}$ represents the AD forces in the wind farm simulation including ADs, and $\widetilde{P}$ represents the fluctuation around the static pressure that is solved by the SIMPLE algorithm [13]. The pressure gradients are obtained as $\partial P/\partial x = \partial \widetilde{P}/\partial x + \rho f_c V_G$ and $\partial P/\partial y = \partial \widetilde{P}/\partial y - \rho f_c U_G$. We are interested in the momentum balance in the cross direction (y), which can be written as:

$$\underset{\text{Change of V-momentum}}{\int_A \frac{DV}{Dt} dA} = \underset{\text{Coriolis}}{-f_c \int_A U dA} \quad \underset{\text{Pressure}}{-\frac{1}{\rho}\int_A \frac{\partial P}{\partial y} dA} \quad \underset{\text{Turbulence}}{-\int_A \frac{\partial \overline{v'w'}}{\partial z} dA} \tag{3}$$

The integrals are taken over square horizontal slices with an area of $A = 40 \times 40D^2$ at several heights, in the wind farm ($x = y = \{-4D, L_{WF} + 4D\}$) and in the near wind farm wake ($x = \{L_{WF}, 2L_{WF}+8D\}$, $y = \{-4D, L_{WF}+4D\}$). The integrals with $\int_A \frac{\partial \overline{u'v'}}{\partial x} dA$ and $\int_A \frac{\partial \overline{v'v'}}{\partial y} dA$ can be neglected because they are 2-3 orders of magnitude smaller than the other integrals from equation 3. In addition, $S_{AD,y} = 0$ since only thrust forces are considered, and the ADs are fixed normal to the flow direction. Each term of equation 3 is normalized by $1/(Af_cG)$ and plotted in Figure 5.

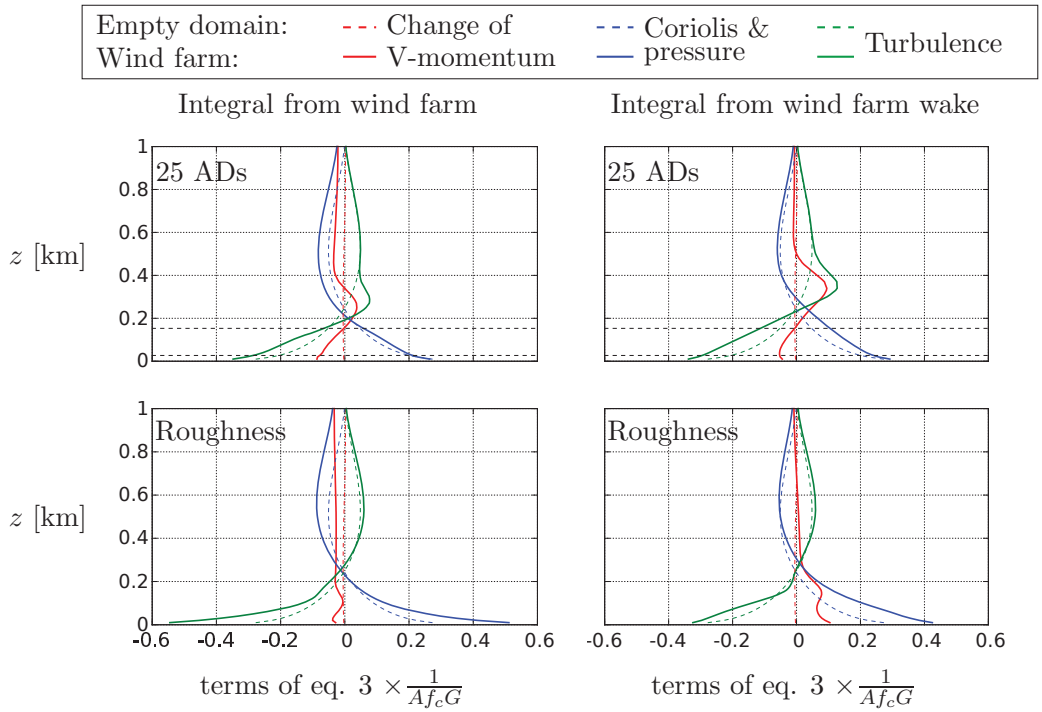

Figure 5. V-Momentum balance. Top: wind farm represented by 25 ADs, where rotor area is shown as black dashed lines. Bottom: wind farm represented by a high roughness. Left: integral taken from wind farm area. Right: integral taken from near wind farm wake. Dashed lines represent the results from an empty domain.

The top and bottom figures show results from the simulation where the wind farm is represented by 25 ADs and a high roughness, respectively. In addition, the results from the left figures are taken inside the wind farm, while the right figures are made in the near wind farm wake. The results from the wind farm simulation (solid lines) are compared with the results taken from a empty domain (colored dashed lines). When the wind farm is not present (colored dashed lines from Figure 5), the turbulence is in balance with the Coriolis force and pressure

gradient, as expected. At the wind farm area (left plots of Figure 5), there is more turbulence developing when the wind farm is represented by ADs (left, top plot) compared to a wind farm represented by a roughness change (left, bottom plot). In the near wind farm wake (right plots of Figure 5), this difference in turbulence between the two wind farm simulations is even more pronounced.

When the wind farm is represented by a high roughness (bottom plots of Figure 5), an internal boundary layer (IBL) develops from the abrupt roughness change at $x/L_{WF} = 0$. The largest changes in turbulence are mainly occurring near the wall due to IBL, where also the largest change of V-momentum in the near wind farm wake (right, bottom plot) is observed. In addition, the near wake (right, bottom plot) shows that the combined change of Coriolis force and pressure gradient is larger than the change of the turbulence. Hence, the local changes in Coriolis force and pressure gradient deflect the wind farm wake towards to left, which is already visible in the wind farm area, as shown by the right plots of Figure 4.

When the wind farm is represented by 25 ADs (top plots of Figure 5), the turbulence and V-momentum change both near the wall and above the wind turbines. In both the wind farm and the near wind farm wake, the change in turbulence is larger than the combined change of Coriolis force and pressure gradient, especially above the wind farm, where also the change of V-momentum in near wind farm wake is the largest. This indicates that the turbulence above the wind farm is transporting flow with a wind direction towards to right, downwards, which causes the wind farm wake to turn to the right. In other words, Figure 5 suggests that the Coriolis force is indirectly causing the wind farm wake to deflect towards the right because of the present wind veer, and not because of the local changes in the Coriolis force as motivated in previous work[1]. It would be useful to confirm these findings by large eddy simulations.

Figure 5 shows that the flow in a simulation with 25 ADs including Coriolis is complex and very different from a simulation modeling a roughness change with Coriolis force. This means that the interaction between the Coriolis force and a wind farm wake cannot be simplified to the interaction between the Coriolis force and a roughness change, when the wake deflection is investigated, as suggested by Mitraszewski[3].

4. Conclusions

Two RANS simulations of a wind farm including the effect of the Coriolis force are carried out, that differ in wind farm representation. When the wind farm is modeled as a roughness change, the wind farm wake turns to the left due to an imbalance in the Coriolis force. When the wind farm is represented by 25 actuator disks, the wind farm wake is deflected towards the right. An investigation of the momentum balance in the cross flow direction suggests that in the simlation with 25 actuator disks, the turbulence is mixing fresh momentum from above, that has a relative wind direction towards the right, down into the wake region. Hence, the interaction between the Coriolis force and a wind farm wake is a complex process that cannot be simplified to the interaction between the Coriolis force and a roughness change, when the deflection of the wind farm wake is investigated.

Acknowledgments

This work is supported by the Center for Computational Wind Turbine Aerodynamics and Atmospheric Turbulence funded by the Danish Council for Strategic Research, grant number 09-067216. Computational resources were provided by DCSC and the DTU central computing facility.

References

[1] van der Laan M P, Hansen K S, Sørensen N N and Réthoré P E 2015 *Journal of Physics: Conference Series* **524** 1
[2] Volker P J H, Badger J, Hahmann A N and Ott S 2015 *Geosci. Model Dev.* **8** 3715
[3] Mitraszewski K S 2012 *Study of the wall effect at offshore wind farms* Master's thesis Technical University of Denmark
[4] Orr A, Hunt J, Capon R, Sommeria J, Cresswell D and Owinoh A 2005 *Weather* **60** 291
[5] Jonkman J, Butterfield S, Musial W and Scott G 2009 Definition of a 5-MW Reference Wind Turbine for Offshore System Development Tech. rep. National Renewable Energy Laboratory
[6] Mikkelsen R 2003 *Actuator Disc Methods Applied to Wind Turbines* Ph.D. thesis DTU
[7] van der Laan M P, Sørensen N N, Réthoré P E, Mann J, Kelly M C and Troldborg N 2015 *Wind Energy* **18** 2223
[8] Sørensen N N 1994 *General purpose flow solver applied to flow over hills* Ph.D. thesis DTU
[9] Michelsen J A 1992 Basis3d - a platform for development of multiblock PDE solvers. Tech. rep. DTU
[10] Apsley D D and Castro I P 1997 *Boundary-Layer Meteorology* **83** 75
[11] van der Laan M P, Sørensen N N, Réthoré P E, Mann J, Kelly M C, Troldborg N, Schepers J G and Machefaux E 2015 *Wind Energy* **18** 889
[12] Sørensen N N, Bechmann A, Johansen J, Myllerup L, Botha P, Vinther S and Nielsen B S 2007 *Journal of Physics: Conference series* **75** 1
[13] Patankar S V and Spalding D B 1972 *International Journal of Heat and Mass Transfer* **15** 1787